Estimation of Wall-Scattering in the Urban Canyon

Antonis G. Dimitriou[1], Stavroula Siachalou[2], George D. Sergiadis[3]

Dept. of Electrical and Computer Engineering, Aristotle University of Thessaloniki
Aristotle University Campus, 54124 Thessaloniki, Greece

[1]antodimi@auth.gr
[2]ssiachal@ad.auth.gr
[3]sergiadi@auth.gr

***Abstract*— Recent measurements have shown that the scattered field from the buildings' façades can greatly affect the magnitude, the delay spread and the angular spread of the received field inside the "urban canyon". In this paper a model that estimates the net scattered field by a single façade is derived, assuming that the building's wall comprises numerous identical elementary scatterers (e.g. windows) with known scattering gain function. The proposed model can be easily implemented in a ray-tracing propagation prediction tool, thanks to its simplicity and the small estimation time.**

I. Introduction

Recently it has been shown through measurements and simulations [1]—[5] that apart from specular reflection, scattering from the buildings' facades might become the dominant propagation mechanism in the "urban canyon". This remark becomes increasingly important nowadays when the development and adoption of sophisticated MIMO systems promises to exploit the "multipath richness" of the wireless channel, increasing the capacity of the communication system.

In [3], the authors define three scattering models and then specify their characteristics from a measurement campaign that is carried out in the vicinity of three walls with different characteristics. Each wall is treated as a single scattering element, even though the models are not subject to such a limitation. As a result, it's impossible to predict the scattering gain at specific orientations in the "urban canyon" due to constructive interference of the scattered field from each individual scatterer on the same wall, as reported in [1].

In [1] the scatterers along the buildings' façades were modeled as two orthogonally arranged series of 90°. The wedges were selected due to their geometrical similarity with the majority of the expected scattering objects [5] and also because their electromagnetic scattering properties have been thoroughly studied. The contribution from discrete scatterers (e.g. windows) located on a single building's façade in a typical microcellular case was recently measured and reported in [4] (see the inclined lines with a down-left to up-right orientation of Fig. 21 in [4]). The measured scattered field is not reproduced in the corresponding simulations because a single scattering coefficient is assumed for each building, implementing the models reported in [3].

In this paper, the effects of scattering by a single building façade in a LOS urban configuration for a transmitting antenna placed well below the average rooftop level are demonstrated and a new model that allows for the calculation of those effects is proposed. Two key assumptions are made. Firstly, the scatterers that are located on the same façade are usually made of the same construction materials and can be considered to have similar scattering behaviour on an impinging EM wave. Secondly, they are spaced by several wavelengths so that scattering by each of them can be treated independently.

The net field is estimated by considering the scattered field by a single scatterer and the phase relations of the scattered components at the receiver. The proposed model is derived for the wedge-scattering model represented in Fig. 1. However, it is shown that the same formulation can be implemented for any elementary scattering function. Applicability of the model is shown in section III for the scattering models presented in [3]. The simplicity and the small estimation-time of the final formulation allow for easy implementation in a ray-tracing propagation prediction tool.

The effects of the scatterers located along a wall in a typical urban configuration are presented in section II. The proposed model is derived analytically in section III.

II. Calculation of the Total Scattered Field for a LOS Configuration

A. Wedge Scattering Model

The façade of the building is replaced by two series of wedges [1], as shown in Fig. 1c. These wedges account for the expected scattering from the actual wedges on the wall, as demonstrated in Fig. 1b. Each of these two series of wedges is responsible for the scattered field that results from the two perpendicular components of the incident electromagnetic field on the wall.

Let's consider the array of vertical wedges, shown in the left part of Fig. 1c. When the receiver moves close to the wall, inside the canyon, the following three regions can be identified with respect to the reflection shadow boundaries (RSBs) of a pair of consecutive wedges, as shown in Fig. 2: *a*) *Region 1*, where the receiver moves in the reflection illumination region (RIR) of wedge 1, in the reflection shadow region (RSR) of wedge 2 and in the reflection region of the wall (RR), *b*) *Region 2* or *Transition Region*, where the receiver moves in the RSR of both wedges and in the reflection shadow region of the wall (there is no reflection), and *c*) *Region 3*, where the receiver moves in the RSR of wedge 1, the RIR of wedge 2 and again in the reflection

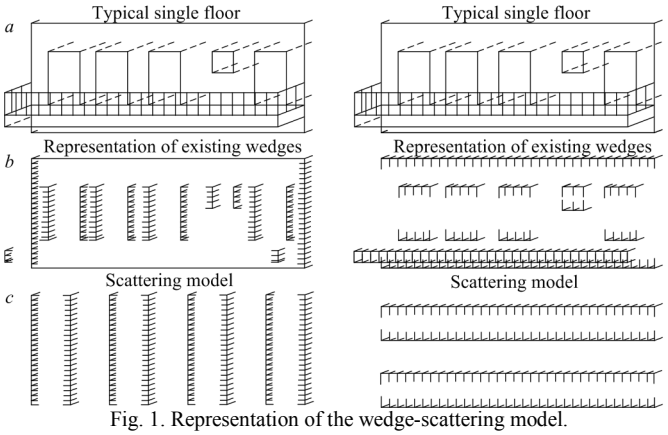

Fig. 1. Representation of the wedge-scattering model.

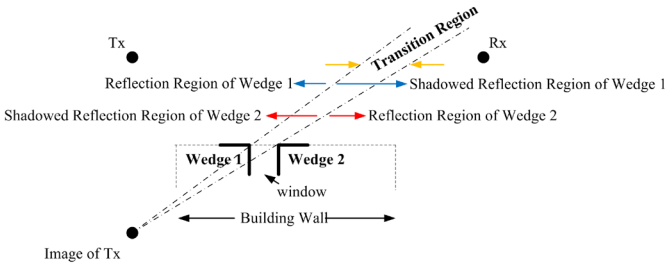

Fig.2 Representation of the area near the RSBs of two consecutive wedges.

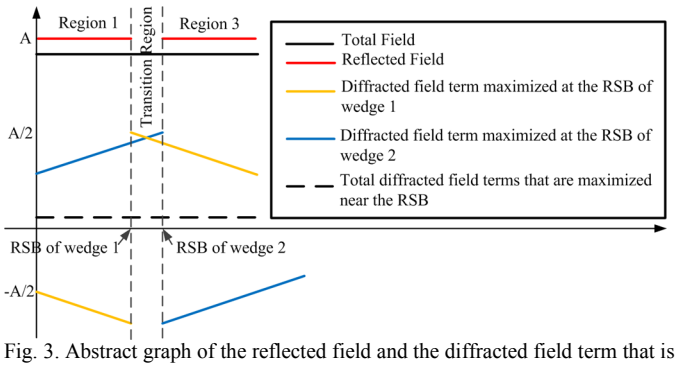

Fig. 3. Abstract graph of the reflected field and the diffracted field term that is maximized close to the RSB.

region of the wall. As the diffraction coefficient term [6]—[7], that is maximized at the RSB changes phase exactly at the RSB of each wedge, so as to ensure continuity of the total field, the total field due to the specific diffraction terms remains almost constant in these three regions, as demonstrated in the abstract graph of Fig. 3. The phase shifts at the RSBs are shown by the discontinuities of the coloured lines, while the sum of the field (black line) remains constant. Of course, in the actual case the total field varies slowly. In order to avoid the extensive search of the location of the receiver with respect to the reflection shadow boundary of each wedge, we consider every pair of wedges at the same coordinates. Consequently, the corresponding RSBs coincide and hence the corresponding terms add destructively. Finally, the reflected field is calculated continuously by the entire wall, as if the transition region of Fig. 2 doesn't exist. This approximation is accurate, while ensuring easy implementation in a ray tracing tool. The same assumption is considered for the other series of wedges, shown in the right part of Fig. 1c.

B. Analysis of the Scattered Field for the Vertical Scatterers

Let's consider a single building inside the urban canyon that comprises an array of vertical wedges as shown in the left part of Fig. 1c. For a 2154MHz frequency (λ=14cm) a pair of wedges is considered every 6m (42λ) along a 50m (357λ) wall. The building is assumed at 150m from the transmitter, which is located in the centre of a 20m width street, well below the average rooftop level. The receiver is assumed at three fixed positions in the centre of the street at a distance of 150m, 200m and 300m from the transmitter respectively. The corresponding times of arrival (TOA) of the scattered rays from each pair of wedges with respect to the time of arrival of the line of sight (LOS) ray are given in Fig. 4 along with the path gain of each component. When the receiver is located before the building, the scattered components arrive with great delays from each other and from the LOS wave. When the receiver is located after the building, the corresponding delays reduce dramatically. For the last position of 300m, all scattered rays arrive within 0.25ns and only 2ns after the LOS contribution. This property becomes particularly important in the calculation of the total scattered field. Due to the small difference in the TOA of the scattered rays and to the nearly identical scattering function by successive pairs of wedges (because the angles of incidence and departure from successive wedges are almost identical), the scattered rays add constructively at the receiver and the net scattered field grows. The phases of the scattered rays that reach the receiver at 300m are plotted in Fig. 5.

In Fig. 6, the total scattered field is calculated versus the LOS field, for a wall at 150m and 300m from the transmitter.

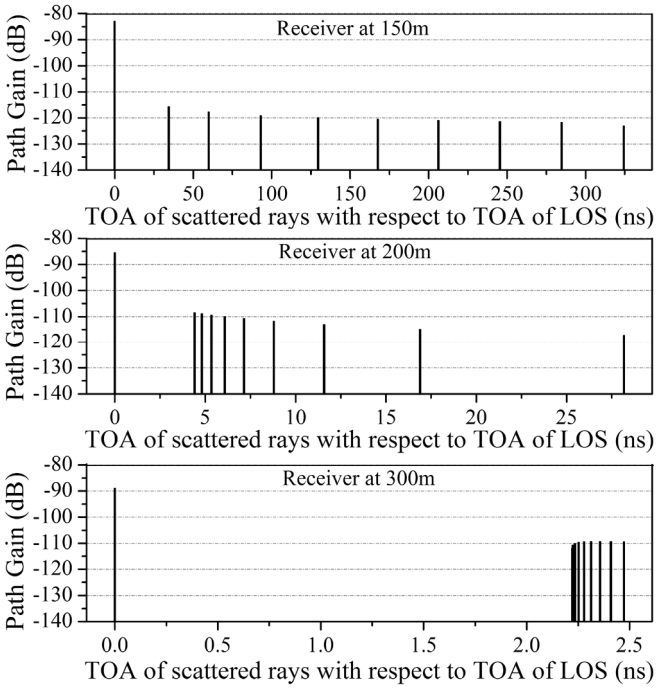

Fig.4. TOA of scattered rays with respect to the TOA of the LOS ray.

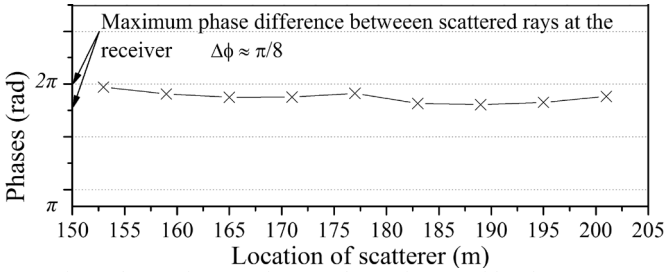

Fig.5. Phases of scattered rays at the receiver considered at 350m.

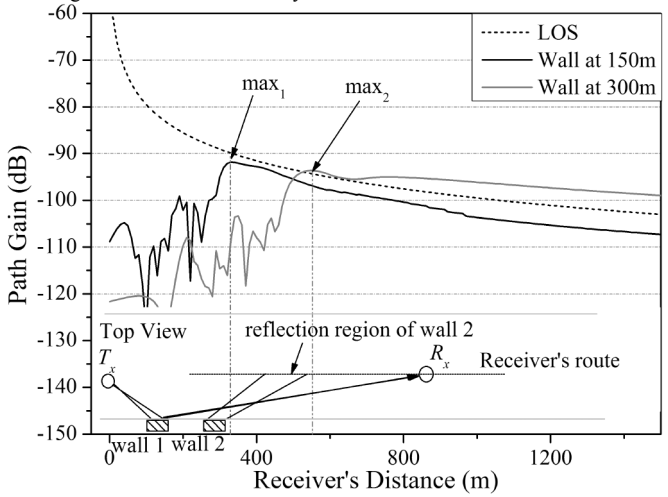

Fig. 6. Scattered field from the vertical wedges.

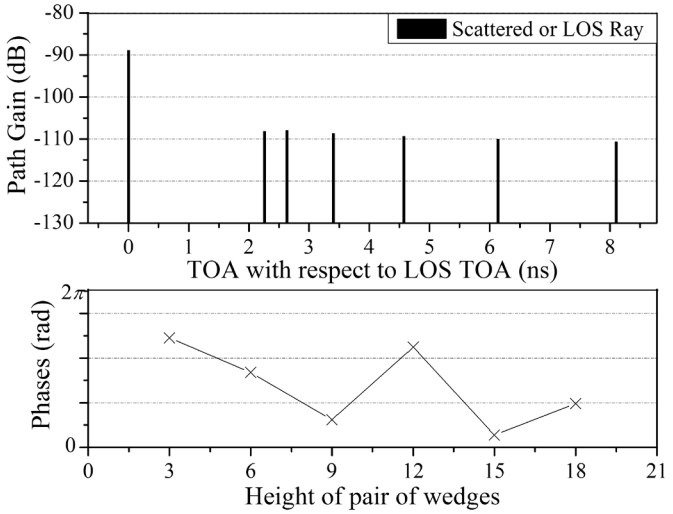

Fig. 7. TOA and phases of the scattered rays at the receiver.

For smaller distances the scattered field is much smaller than the direct. After the receiver crosses the wall, the fast fading gradually shrinks, because the scattered components add constructively at the receiver, as explained above. After reaching a maximum value near the reflection region of the wall, the scattered field starts to fade at a slope similar to the one of the LOS field.

C. Analysis of the Scattered Field for the Scatterers with Axes Parallel to the Ground

The other series of wedges, presented in the right part of Fig. 1c, is now considered. Each pair of wedges is considered every 3m (21λ) for a 21m tall building (6-storey building). The TOA and the phases of the scattered rays are plotted in Fig. 7 for the receiver at 300m. Again, the delays between the scattered rays are small, but not that small to result in constructive interference at the receiver. As a consequence, the total scattered field remains much smaller than the LOS field in the entire street, as shown in the corresponding plot of Fig. 8. However, this array of wedges is responsible for the cross polarized component of the field at the receiver. This component could be of importance in a MIMO system. One could expect a cross polarized component approximately 10dB smaller than the co-polarized one in the entire street. In the same plot the scattered path gain "average" and "proposed" curves that almost coincide will be explained in the following section.

III. Derivation of the Proposed Scattering Model

Let's consider the array of vertical wedges shown in the left part of Fig. 1c. The total scattered field at the receiver is given as the phase-sum of the field resulting from each pair of wedges E_k:

$$E = \sum_{k=1}^{N} E_k e^{j\phi_k} \qquad (1)$$

When the building is located between the receiver and the transmitter and the angles of incidence and departure of the rays from the different scatterers along the building's façade are small (Fig. 6), the magnitudes of the electric field of the diffracted components E_k that reach the receiver are almost equal. In such cases the corresponding phases of the diffracted rays depend only on the path lengths R_k of those rays with respect to the wavelength of operation. These properties were demonstrated in Figs. 5 and 6. The power from each pair of wedges is approximately 20dBs smaller than the LOS contribution. The maximum phase difference of the scattered rays is less than $\pi/8$. As a result the scattered rays add constructively at the receiver and the net scattered field becomes comparable to the LOS contribution. In such a case the magnitude of the total scattered field can be approximated as:

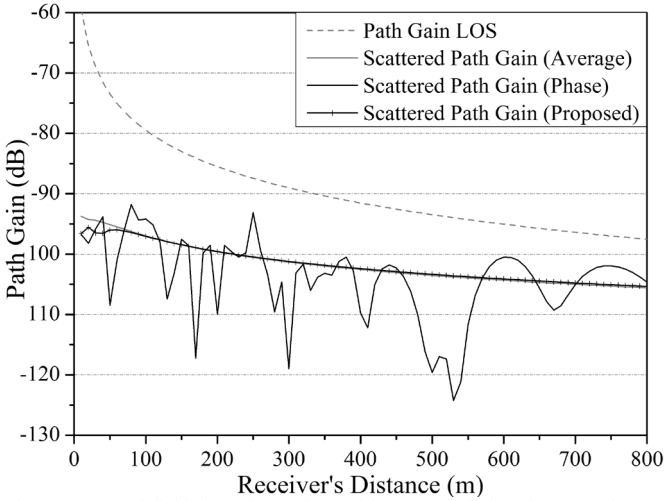

Fig. 8. Scattered field from the wedges with axes parallel to the ground versus the LOS field inside the street.

$$\left|E_{prop}\right| = \left|E_D\right| \left| \sum_{k=1}^{N} e^{j\phi_k} \right| \qquad (2)$$

where E_D is the diffracted field by a pair of wedges located at the centre of the building, N is the number of pairs of wedges along the façade. The upper limit of the phase-sum in (2) is N, which results when all scattered rays add constructively at the receiver. The corresponding lower limit is 0 which results when all contributions add destructively, cancelling out each other in an ideal theoretical manner. The values of the sum between 0 and N depend on the difference in the phases of the scattered components. In order to derive a physically-meaningful approximation of (2), the phase difference of the arriving rays must be taken into account. Taking the above remarks into account, (2) is expressed as the product of N with a function $f(\Delta\varphi)$ that evaluates the phase correlation of the diffracted components that reach the receiver, as explained below. The function $f(\Delta\varphi)$ varies between 0 and 1:

$$\left|E_{prop}\right| = f\left(\Delta\phi\right)\left|E_D\right| N \qquad (3)$$

where $\Delta\varphi$ is the maximum phase difference between any two diffracted components from the same façade $\Delta\phi = \max\left(\left|\phi_k - \phi_m\right|\right)$. $\Delta\varphi$ equals the phase difference between the scattered ray from the specular-reflection-point on the façade and one of the two scattered rays from the two edges of the building (Fig. 6). Thus, $\Delta\phi = 2\pi\left|\Delta R\right|/\lambda$, where ΔR denotes the difference of the distance travelled by the two rays. If the specular reflection point is not on the building's facade then $\Delta\varphi$ equals the phase difference between the scattered rays from the two edges of the building.

Naturally, for $\Delta\varphi\rightarrow 0$, $f(\Delta\varphi)\rightarrow 1$. When the phases of the arriving rays are entirely uncorrelated, they can be considered uniformly distributed in $(0,2\pi)$. In such a case, it can be shown that the mean of the square of the sum of N rays of equal magnitude with random phases uniformly distributed in $(0,2\pi)$ as given in (2) equals $|E_D|^2 N$. Therefore, for greater values of $\Delta\varphi$, say $\Delta\varphi > 2\pi$, one can assume $f(\Delta\varphi)\rightarrow 1/\sqrt{N}$. In Fig. 9, the actual values of $f_{est}(\Delta\varphi)$ for N=9 are plotted, where:

$$f_{est}\left(\Delta\phi\right) = \frac{\sum_{k=1}^{N} E_k e^{j\phi_k}}{N\left|E_D\right|} \qquad (4)$$

As shown in Fig. 9, $f_{est}(\Delta\varphi)$ can be well approximated by a function in the following form:

$$f\left(\Delta\phi\right) = a + \frac{b}{1 + c^{(\Delta\phi - \pi)}} \qquad (5)$$

Parameter a is defined by the desired value for greater values of $\Delta\varphi$, hence $a=1/\sqrt{N}$. Parameter c is defined by the desired slope of the function for $\Delta\phi \in (0,\pi)$ and b is defined by the desired behaviour for $\Delta\varphi$=0 ($f(0)$=1). Parameter c has been found to vary between 3 and 4 for increasing N in an S-shape manner. Hence a generalized logistic function is expected to fit well the variation of c [8]. An alternative could be the use of the Gombertz function [9]. The parameters of the logistic function were selected so as to fit the desired asymptotes and the variation of c. Parameter c is given in the following formula:

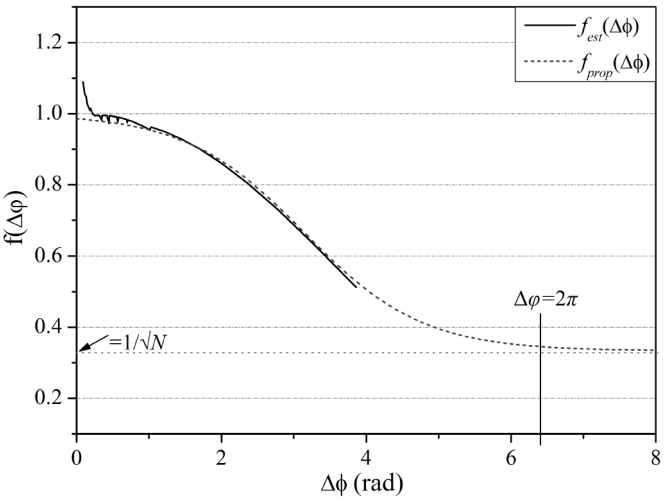

Fig. 9 Comparison between $f_{est}(\Delta\varphi)$ given in (4) and $f_{prop}(\Delta\varphi)$ given in (7).

$$c = 3 + \frac{1}{1 + e^{4 - 0.4N}} \qquad (6)$$

Therefore $f(\Delta\varphi)$ is given as:

$$f_{prop}\left(\Delta\phi\right) = \frac{1}{\sqrt{N}} + \frac{\left(1 - \frac{1}{\sqrt{N}}\right)\left(1 + c^{-\pi}\right)}{1 + c^{(\Delta\phi - \pi)}} \approx \frac{1}{\sqrt{N}} + \frac{\left(1 - \frac{1}{\sqrt{N}}\right)}{1 + c^{(\Delta\phi - \pi)}} \qquad (7)$$

The function $f_{prop}(\Delta\varphi)$ is plotted in Fig. 9 and demonstrates good agreement with $f_{est}(\Delta\varphi)$, given in (4) for N=9. Similarly accurate results were recorded for different values of N. By first substituting (6) to (7), and then (7) to (3), the diffracted field is given as

$$\left|E_{prop}\right| = N\left[\frac{1}{\sqrt{N}} + \frac{\left(1 - \frac{1}{\sqrt{N}}\right)}{1 + \left[3 + \frac{1}{1 + e^{4 - 0.4N}}\right]^{(\Delta\phi - \pi)}}\right]\left|E_D\right| \qquad (8)$$

and the corresponding path gain in dB:

$$PG^{prop}\left(dB\right) = 10\log_{10}\left(\frac{\lambda^2}{4\pi}\frac{1}{2\eta}\left|E_{prop}\right|^2\right) \qquad (9)$$

where λ is the wavelength of operation, η the characteristic impedance of free-space.

A. Comparative Results for the Vertical Wedges

The path gain using the proposed approximation (9) is compared with the path gain of the diffracted field in Fig. 10, assuming the building at 300m, given by:

$$PG^{phase}\left(dB\right) = 10\log_{10}\left[\frac{\lambda^2}{4\pi}\frac{1}{2\eta}\left|\sum_{k=1}^{N} E_k e^{j\phi_k}\right|^2\right] \qquad (10)$$

where E_k is the magnitude of the electric field of the scattered component k, and φ_k its phase. Assuming that the phases of the multipath components are considered random variables uniformly distributed in $(0,2\pi)$, the mean of the path gain,

plotted in Fig. 10, is proportional to the sum of the square of the electric field of the individual components:

$$PG^{avg}(dB) = 10\log_{10}\left[\frac{\lambda^2}{4\pi}\frac{1}{2\eta}\sum_{k=1}^{N}|E_k|^2\right] \qquad (11)$$

As demonstrated, for small distances, the proposed approximation (9) accurately estimates the expected mean scattered power. Then, for greater distances (w>500m), the proposed equation approximates well the phase sum of the scattered power that reaches the receiver. Therefore, by implementing (8), one can accurately estimate the total scattered field from the façade of a building with N identical scatterers, by simply calculating the contribution of a single scatterer and the maximum phase difference between any two scattered rays that reach the receiver due to the corresponding different path lengths. The success of (8) is that, by taking into account the phase relations of the scattered rays, it estimates the expected value of the scattered field anywhere inside the street. Similar behaviour was recorded for a building at 150m and 450m.

B. Comparative Results for the Horizontal Wedges

The corresponding graph was presented in Fig. 8. The proposed formula follows the mean expected power, as the scattered rays do not add constructively, due to the greater differences between the path lengths of the scattered rays.

C. Comparative Results for a Different Scatterer

Finally, in Fig. 11 the proposed formulation is used, assuming a different scattering gain function. Specifically, the single lobe model with the best fit parameters derived in [3] was implemented. We considered $K=dS/dS_{elem}$ equally spaced scatterers of surface dS_{elem}=2m×2m on a wall of surface dS=50m×30m. The proposed formulation PG_{elem} is compared with the path gain assuming the entire wall as a single scatterer (PG_{wall}) of surface dS and also by calculating the phase sum of the scattered field by each elementary scatterer, by implementing (10) using the model derived in [3]. Again for small distances PG_{elem} predicts the average scattered field by the entire wall, while for greater distance it estimates the phase sum of the field by the array of scatterers.

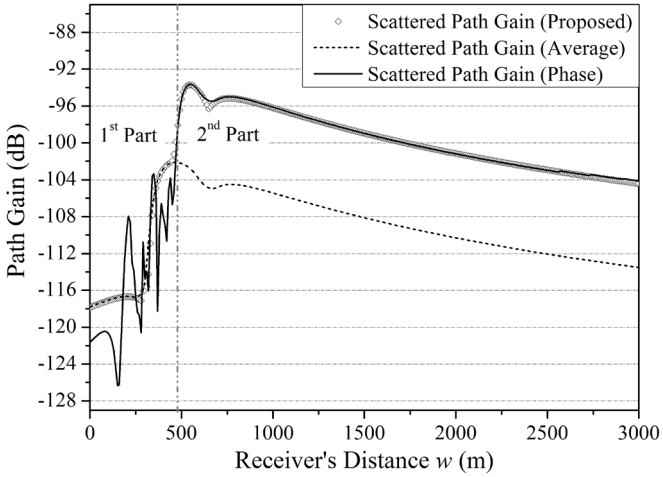

Fig. 10. Estimated scattered field using the proposed formulation vs. the analytical.

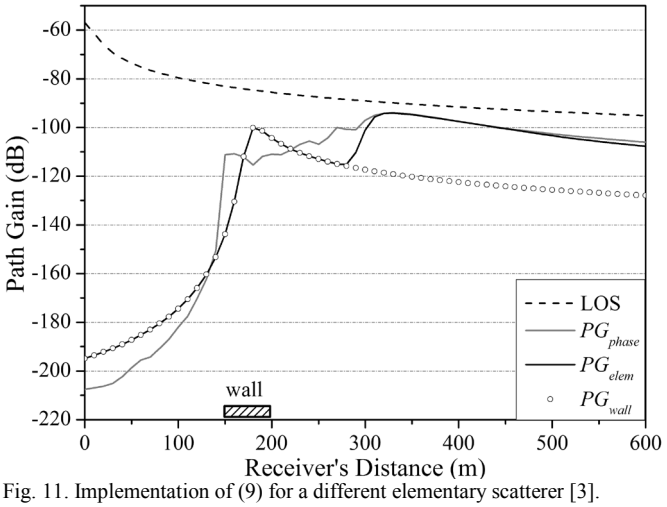

Fig. 11. Implementation of (9) for a different elementary scatterer [3].

IV. CONCLUSIONS

In this paper, a new model is derived that allows for the calculation of the scattered field inside an "urban canyon", caused by identical elementary scatterers located on a single building's façade. The model is suitable for typical urban microcells. The scattered field is estimated by calculating the maximum phase difference of the field by any pair of scatterers located on the same wall and the scattered field by a scatterer located in the centre of the wall. Any scattering gain function can be implemented in the model. Proper spacing of the scatterers should be selected based on the actual configuration of the selected environment. For a Mediterranean-style urban environment, it is suggested to consider a pair of wedges every 6m.

REFERENCES

[1] A. G. Dimitriou and G. D. Sergiadis, "Architectural features and urban propagation," *IEEE Trans. Antennas Propagat.*, vol. 54, no. 3, pp. 774-784, March 2006.

[2] V. Degli-Esposti, D.Guiducci, A. de' Marsi, P. Azzi, and F. Fuschini,"An advanced field prediction model including diffuse scattering," *IEEE Trans. Antennas Propag.*, vol. 52, no. 7, July 2004.

[3] V. Degli-Esposti, F. Fuschini, E. M. Vitucci, G. Falciasecca "Measurement and modelling of scattering from buildings," *IEEE Trans. Antennas Propag.*, vol. 55, no. 1, pp. 143–153, Jan. 2007.

[4] F. Fuschini, H. El-Sallabi, V. Degli-Esposti, L. Vuokko, D. Guiducci, and P. Vainikainen, "Analysis of multipath propagation in urban environment through multidimensional measurements and advanced ray tracing simulation," *IEEE Trans. Antennas Propagat.*, vol. 56, no. 3, pp. 848-857, March 2008.

[5] H. Budiarto, K. Horihata, K. Haneda, and J. Takada, "Polarimetric measurement of nonspecular wave scattering from building surface roughness," *IEEE Antennas and Wireless Propagat. Letters*, vol. 2, pp. 242—245, 2003.

[6] R. G. Kouyoumjian and P. H. Pathak, "A uniform geometrical theory of diffraction for an edge in a perfectly conducting surface," *Proc. IEEE*, vol. 62, no. 11, pp. 1448-1461, Nov. 1974.

[7] R. J. Luebbers, "Finite conductivity uniform GTD versus knife edge diffraction in prediction of propagation path loss," *IEEE Trans. Antennas Propagat.*, vol. 32, no. 1, pp. 70-76, Jan. 1984.

[8] F.J. Richards, "A flexible growth function for empirical use," *Journal of Experimental Botany*, vol. 10, pp. 290—300, 1959.

[9] B. Gompertz, "On the nature of the function expressive of the law of human mortality, and on a new mode of determining the value of life contingencies," *Philosophical Transactions of the Royal Society of London*, Vol. 115, pp. 513-585, 1825.